

Characterization of a novel hybrid silicon three-axial force sensor

P. Valdastrì^{a,*}, S. Roccella^b, L. Beccai^a,
E. Cattin^b, A. Menciassi^a, M.C. Carrozza^b, P. Dario^{a,b}

^a CRIM (Centre for Research In Microengineering), Polo Sant'Anna Valdera – Scuola Superiore Sant'Anna,
Viale Rinaldo Piaggio 34, 56025 Pontedera (PI), Italy

^b ARTS Lab (Advanced Robotics Technology and Systems Laboratory), Polo Sant'Anna Valdera –
Scuola Superiore Sant'Anna, Viale Rinaldo Piaggio 34, 56025 Pontedera (PI), Italy

Received 3 September 2004; received in revised form 16 December 2004; accepted 9 January 2005

Available online 10 February 2005

Abstract

A three-axial silicon based force sensor with a volume less than 7 mm^3 , developed for biomechanical measurements, has been characterized. Results obtained with two different experimental test benches are reported in this paper. High linearity and low hysteresis during sensor normal loading have been obtained by using a preliminary test bench. A second improved test bench, based on a six-components load cell, has been employed to perform a reliable sensor calibration. A sensitivity matrix has been evaluated from experimental data and an estimation of force accuracy has been determined. The experimental sensitivity in the shear directions is 0.054 N^{-1} and in the normal direction is 0.026 N^{-1} . A method for comparing the device characteristics with similar state of the art three-axial force sensors has been provided.

© 2005 Elsevier B.V. All rights reserved.

Keywords: Three-axial force sensor; Hybrid; Characterization; MEMS-based

1. Introduction

A novel hybrid silicon three-axial force sensor has been developed for biomechanical measurements in the field of prosthetics, in particular in order to address the problem of the bad fitting of the socket to the stump in lower limb above-knee (AK) amputees [1–3]. The device has been designed in order to develop a flexible smart interface to be used to detect the entity and distribution of normal and shear forces that arise, during user locomotion, at the interface between the socket surface and the stump. This measurement can be used to evaluate the fitting degree of the socket and to optimize its shape, thus reducing the skin damage. In addition, the mechanical characteristics of the sensor have also been assessed as appropriate for the sensory system of artificial hands [4,5].

In this paper the characterization of the three-axial silicon based force sensor is presented. Particular attention has been devoted to methods used in literature to approach the same problem. Multi-component and shear force sensors have been developed in silicon and in other materials including aluminum and steel, mainly using the piezoresistive transduction. The main features of a selection of multi-component miniaturized force sensors and the characterization methods used are summarized in Table 1.

Concerning the calibration methods, mostly a mono-axial load cell is the core component of the calibration system, despite of the low accuracy for a multi-axial calibration. An alternative solution, reported in [15], is to use a system of weights suspended from the tip of the sensor, but this is unsuitable if the sensors dimensions become smaller than few centimeters. In [17] a solution for planar multi-component, microforce sensor calibration is proposed: an aluminum cross-beam is suspended over and connected to the sensor structure at the beams' centers. During calibration, the sensor is placed in a magnetic field and current is

* Corresponding author.

E-mail address: pietro@sss.it (P. Valdastrì).

Table 1
Comparisons on principal multi-component miniaturized force sensors

Device	Descriptions	Fabrication technology	No. of axes	Size (mm)	Sensitivity	Force range	Characterization method
Mei et al. [6]	Array of 4×8 individual sensing elements, piezoresistive principle	CMOS process, silicon bulk micromachining, epoxy assembling	3	$4 \times 4 \times 1.5$	13 mV N^{-1} in Z, 2.3 mV N^{-1} in X and Y	50 N in Z, 10 N in X and Y	Three components load cell
Jin and Mote [7]	Planar cross shape structure, without force concentrating structure, piezoresistive principle	Silicon bulk micromachining, Si–Au eutectic bonding	6	$4.5 \times 4.5 \times 1.2$	18.8 mV N^{-1} in Z ^a , 2.41 mV N^{-1} in X ^a , 2.01 mV N^{-1} in Y ^a	n.a.	Purposely developed three components test bench [17]
Dao et al. [8]	Planar structure, piezoresistive principle	Silicon micromachining by DRIE	6	$3 \times 3 \times 4$	1.15 V N^{-1} in Z, 0.11 V N^{-1} in X and Y	n.a.	Mono-axial load cell
Wang and Beebe [9]	SU8 square mesa, piezoresistive principle	Silicon bulk micromachining, soft lithography	3	Diaphragm: $1.9 \times 1.9 \times 0.05$, mesa: H 0.6	1.57 N^{-1} in Z ^b , shear sensitivity varies with loading conditions	3 N	Mono-axial load cell
Bütefish et al. [10]	Stylus fixed by epoxy resin, piezoresistive principle	Silicon bulk micromachining	3	$5 \times 5 \times 0.36$	0.36 N^{-1} in Z ^c , 13.2 N^{-1} in X and Y ^c	n.a.	Mono-axial load cell
Hsieh et al. [11]	Sensitive to shear forces (SiO ₂ flange), piezoresistive principle	Silicon bulk micromachining	2	$3 \times 3 \times 0.3$	0.13 mV (mA MPa) in X and Y	44 N	Mono-axial load cell
Kane et al. [12]	Array of 64×64 individual sensing elements with planar structure, piezoresistive principle	CMOS process, silicon bulk micromachining	3	Array: 19.2×19.2	1.59 mV kPa^{-1} in Z, 0.32 mV kPa^{-1} in X and Y	35 kPa in Z, 60 kPa in X and Y	Purposely developed set-up, with a mono-axial load cell and a differential pressure sensor
Chu et al. [13]	Array of 3×3 individual sensing elements, capacitive principle	Silicon micromachining by electrochemical etching, glass etching, anodic bonding, elastomeric packaging	3	Array: $10 \text{ mm} \times 10 \text{ mm}$	0.13 pF g^{-1} in Z, 0.32 pF g^{-1} in X and Y	1 g	Mono-axial load cell
Chi and Shida [14]	Multifunctional sensing technique	n.a.	3	$\varnothing 15 \text{ mm}$, H 40 mm	$0.18 \text{ } \mu\text{H N}^{-1}$ in Z, shear force: 5.1 mV N^{-1} (amplitude), 0.002 pF° (angle)	4.9 N in Z, 11.76 N in X and Y	Mono-axial load cell
Berkelman et al. [15]	Stainless steel structure with commercial silicon strain gauges	Wire EDM, manual assembly	3	$\varnothing 12.5 \text{ mm}$, H 15 mm	14.12 V N^{-1} in Z ^d , 16.92 V N^{-1} in X ^d , 17.13 V N^{-1} in Y ^d	$\pm 1 \text{ N}$	Weight system

Table 1 (Continued)

Device	Descriptions	Fabrication technology	No. of axes	Size (mm)	Sensitivity	Force range	Characterization method
Diddens et al. [16]	Aluminum structure with commercial silicon strain gauges	Standard aluminum mechanical drilling, manual gluing of strain gauges	3	\varnothing 12 mm, H 20 mm	8.2 mV N ⁻¹ in Z ^d , 7.2 mV N ⁻¹ in X ^d , 7.8 mV N ⁻¹ in Y ^d	100 MPa	n.a.

Symbols: H, height; \varnothing , diameter.

^a Values extracted using definitions (5)–(7) from the transformed sensitivity matrix in [7].

^b The normal sensitivity is given as the ratio of fractional resistance variation to the corresponding force. The indicated value is the highest one, as reported from [9].

^c The sensitivities normalized to the full range voltage value from [10].

^d Highest values extracted using definitions (5)–(7) by the authors from the transformed sensitivity matrix, evaluated applying the *pinv* Matlab[®] instruction (that computes the Moore-Penrose pseudoinverse) to the sensitivity matrix, from [15] and [16] without permission.

driven through the aluminum beams to produce a Lorentz force. By selecting the magnetic field and the current, electromagnetic forces with known magnitudes and directions are generated. This calibration system was used to calibrate a six-component silicon microforce sensor, as reported in [7]. Major limitations of this technique rely on the planar structure of the calibration device, thus it does not appear to be suitable to force sensors that have an out of plane force concentrating structure.

The three-axial force sensor characterized consists of two parts: a sensing chip and a carrier chip, connected together by flip-chip bonding. The sensing part, represented in Fig. 1, is a silicon high aspect-ratio structure with an integrated silicon mesa used for the transmission of the force to a flexible tethered structure. Four bar shaped p-type piezoresistors, integrated at the tether roots are used independently in order to measure the three components of an applied force through a resistance change.

Fabrication of the sensor has been carried out through a 9-mask process by applying Advanced Silicon Etching (ASE) technology to both device and handle layers of a (1 0 0) n-

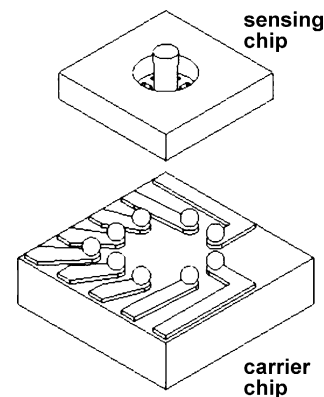


Fig. 2. Sensor assembly by flip-chip technique.

type SOI wafer [3]. The p-type piezoresistors are obtained by ion implantation in the device layer.

The sensor is bonded with conductive glue to a carrier chip, as illustrated in Fig. 2. The final sensor dimensions are 2.3 mm \times 2.3 mm \times 1.3 mm. Skin-like layers are considered for the packaging to ensure a suitable interface between the sensor and the human body [2].

In this work we present the sensor characterization results obtained by two types of systems: one including a mono-axial load cell, described in Section 2.1, and one including a six-components load cell described in Section 2.2. Experimental results obtained by means of both systems are reported in Section 3 and discussed in Section 4.

2. Characterization methods

The sensor has been tested with a preliminary experimental test bench, whose core component is a mono-axial load cell. Such a system allows to test the linearity of response and sensor hysteresis, nevertheless it does not allow to obtain a reliable sensitivity matrix since loading force vector can be acquired only for one of its three directions. Therefore a second measurement system has been purposely developed

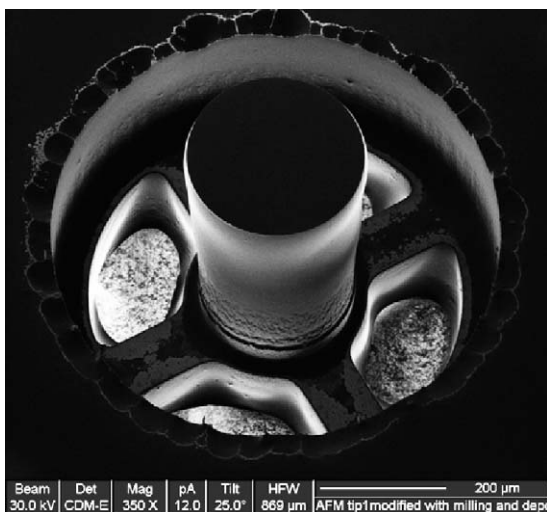


Fig. 1. Focused ion beam (FIB) view of the mechanical sensor structure.

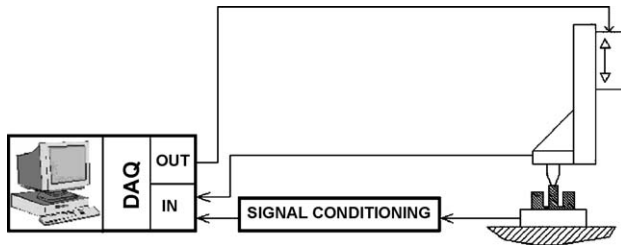


Fig. 3. Schematic diagram of the preliminary test bench.

which exploits a six-components load cell for the complete characterization of the sensor.

2.1. Preliminary test bench description

The preliminary characterization apparatus, sketched in Fig. 3, consists of a loading structure, a double vision system for indenter-sensor alignment, signal conditioning electronic circuitry, data acquisition, and a PC workstation for data analysis.

The load is applied to the sensor by a needle shaped end-effector, screwed to the final part of a subminiature load cell, Model 11 (full scale of 1 kg) from Sensotec (Columbus, OH, USA). This loading structure is mounted on a servo-controlled nanometric translation stage, with a dc servomotor (111-1DG, PI, Karlsruhe, Germany), that imposes a force on the sensor mesa, with a user defined speed. The dc motor is equipped with a high resolution encoder featuring a resolution of 7 nm per step and is connected to a controller (PI Mercury C-860.10) that is interfaced to the PC workstation.

The nanometric slider is fixed on x - y - z manual micrometric translation stage (M-105.10, PI, Karlsruhe, Germany), for rough positioning. This loading system is suitable for both normal and tangential load, just by changing the orientation of the nanometric stage on the rough positioning system.

The sensor device is wire-bonded to a purposely developed steel support, which possesses an air suction system in order to keep the sensor in a stable position during loading tests.

The alignment between the loading structure and the sensor mesa is performed using two fiber optic microscopes: VH5901 with 50 \times magnification from Keyence (Woodcliff Lake, NJ, USA) for alignment in x direction, and KH2700 with 50 \times magnification from Hirox (Tokyo, Japan) for alignment in y direction.

The conditioning electronics have been designed in order to have an output voltage proportional to the fractional change in resistance $\Delta R/R$. Each resistor ($R \cong 1 \text{ k}\Omega$) is independently conditioned, using a quarter Wheatstone bridge configuration with two precision 1 k Ω resistors and one trimmer, in order to adjust the initial offset level. The bridge output signal is then connected to an instrumentation amplifier (AD620, Analog Devices, Norwood, MA, USA). The amplifier gain A can be adjusted from 1 to 1000. The input voltage of the Wheatstone bridge is set to $V_{IN} = 3.3 \text{ V}$ in order to obtain stable output signals without overheating the strain gauges.

Considering a balanced bridge where $R_1 = R_2 = R_3 = R_4 = R$, the output of the circuit is

$$V_{OUT} = A(V^+ - V^-) = AV_{IN} \frac{\Delta R}{4R + 2\Delta R} \approx AV_{IN} \frac{\Delta R}{4R} \quad (1)$$

Thus the resistance variation can be obtained from the output voltage. The four amplified signals from the sensor piezoresistors are acquired with a DAQ (Data Acquisition) Card (NI 6062E, from National Instruments, Austin, TX, USA). The instrumentation amplifier gain of each channel is selected in order to fit the input dynamic of the DAQ Card.

The operator, through a graphical user interface purposely developed using LabView 7 Express (National Instruments, Austin, TX, USA), can apply a translation to the nanometric slider, and thus load the sensor while sampling the four sensor channels and the load cell output.

2.2. Final test bench description

The main difference between the preliminary and the current characterization system is related to the loading station. It has been designed in order both to improve the stability of the sensor mounting, while applying the normal and shear forces, and to measure magnitude and direction of the applied loads with a six-components load cell. This loading station consists of two sub-modules, as illustrated in Fig. 4: the loading system, with the rough and the fine positioning units, and the sensor support.

The loading system exploits three micrometric translation stages with crossed roller bearing (A) (M-105.10, PI, Karlsruhe, Germany), that allow a rough positioning of the loading structure close to the sensor under test. Contact between

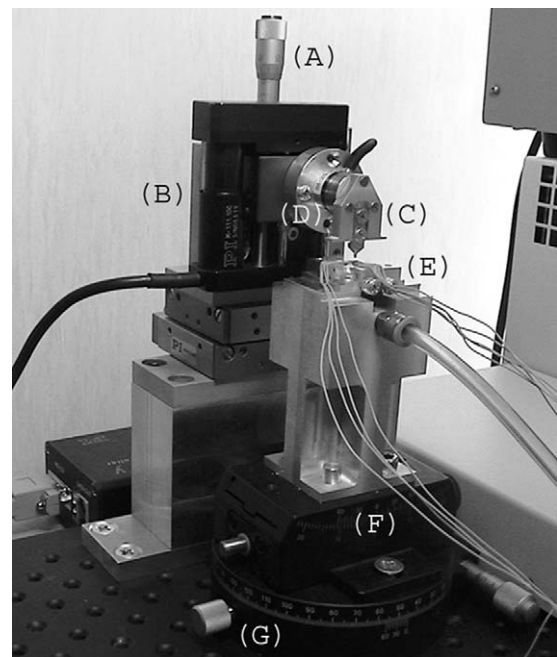


Fig. 4. Global view of the loading station.

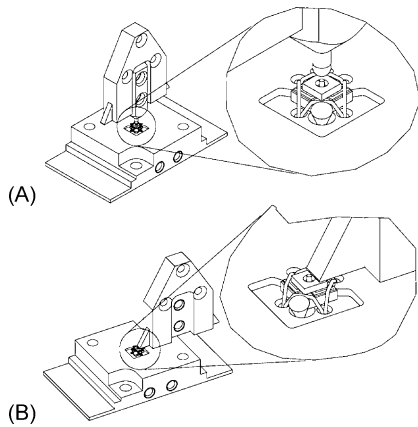


Fig. 5. Schematic drawing of normal (A) and tangential (B) loading.

this part and the sensor is obtained by a servo-controlled nanometric translation stage (B) (M-105.10, PI, Karlsruhe, Germany), in order to finely control the testing cycle. The loading structure (C) is composed by a normal and a tangential loading ends. The normal probe is used to load the sensor in normal direction, as in Fig. 5A, and it consists of a high precision sphere (diameter of 1 mm), fixed by an epoxy glue to a support. This is mechanically coupled with the tangential probing unit, which exploits two lateral plane appendices in order to apply a shear force to the sensor, as represented in Fig. 5B. All the components of the probe system are made of aluminum.

An important design issue that has been considered was to guarantee a point contact between the loading end and the sensor mesa, in order to avoid unwanted misalignments. When a normal force is applied, the contact occurs between the sphere and the mesa upper surface, which is flat, thus achieving the punctual loading. Moreover when a shear force is applied, the flat lateral end of the loading structure touches

the lateral surface of the cylindrical mesa, thus a contact along a line is obtained.

In order to measure and record both magnitude and direction of the force applied to the microsensor, a six-components load cell (D) (ATI NANO 17 F/T, Apex, NC, USA) is placed at the interface between the loading structure and the nanometric translation stage. The use of a multi-component load cell is a key issue in the design of a test bench for the characterization of a multi-dimensional sensor, in order to record also the undesired force components introduced by the non-perfect alignment between the loading structure and the sensor that is unavoidable in a real set-up. Moreover, by using all these information it would be possible to evaluate the sensitivity matrix without the approximations needed if a mono-dimensional load cell was used.

Regarding the sensor support, the silicon device is placed in an aluminum housing (E) that has been fabricated using a 5-axis CNC machining centre, in order to ensure a stable and high precision positioning of the silicon chip. The sensor is placed on a planar surface bounded by two reference points located at two adjacent sides of the chip. To avoid sensor lifting while a shear load is applied, air suction is performed through a hole with a diameter of 1 mm connected to a vacuum pump. Four nylon cables (0.08 mm in diameter) are inserted through four holes and are used to fix the sensor at its corners, as shown in Fig. 6. Every cable is screwed to provide correct tensioning. In this way the cable is positioned between the sensor pads, leaving enough space to allow wire bonding to two bondable terminals strips, glued on the support, for the signal connection to the data acquisition system. In order to further block the sensor, a conical PVC wedge is placed by insertion in a cavity obtained by drilling at one of the chip free corners.

The sensor support is placed over a goniometer (F) and rotation stage (G). The goniometer allows the alignment of the indenter axis with the one of the sensor. All the supporting

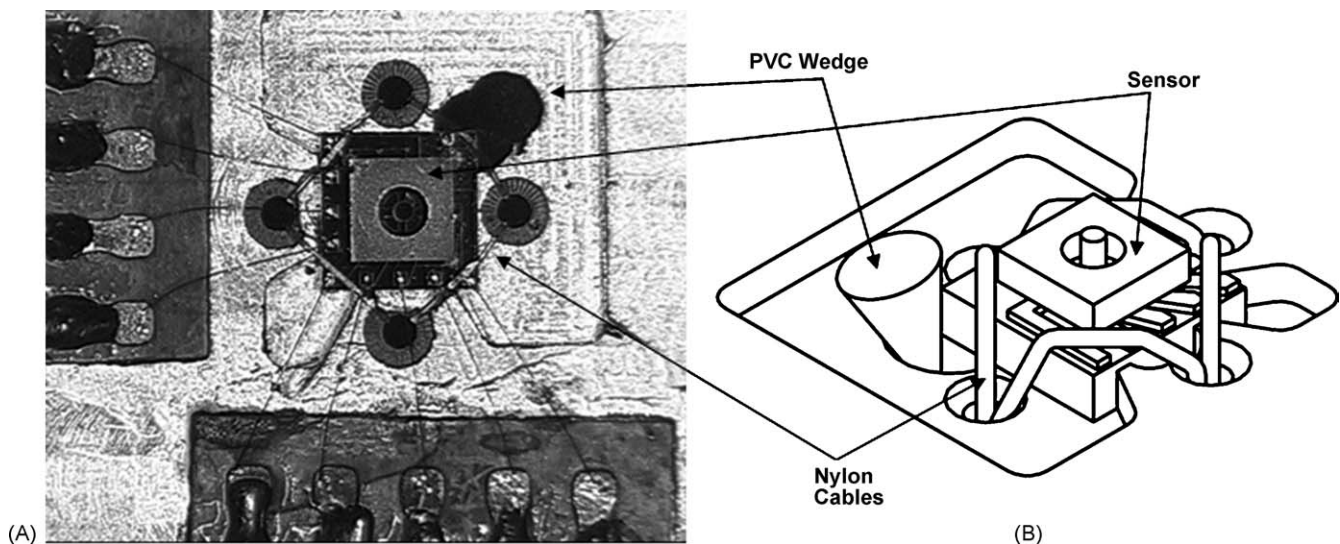


Fig. 6. Top view (A) and schematic lateral view (B) of the sensor fixed to the support.

system has been designed in order to align the upper side of sensor to the goniometer rotation center. The rotation stage allows to rotate the sensor in order to apply shear loads from different angles during the calibration tests.

3. Experimental results

In order to evaluate the hysteresis and the linearity of the sensor, normal loading tests have been performed using the preliminary test bench.

A typical hysteresis cycle, obtained when an applied force increases up to 2 N, considered as a safe load range, and decreases back to zero at a translational constant speed of $1 \mu\text{m s}^{-1}$ along the z direction, has been imposed. Each measurement has been repeated five times to test the reliability of the system.

Typical sensor outputs, in terms of fractional change in resistance $\Delta R/R$ versus loading force are plotted in Fig. 7. Fig. 8 shows the absence of hysteresis during a typical loading cycle for one piezoresistor. The coefficient of determination, which quantifies the linearity of the curve as it is close to 1, is found to be 0.997 for all the piezoresistors outputs.

A calibration procedure is needed to evaluate a linear matrix transform between the piezoresistors bridge signals and the three-component force load vector. To obtain reliable sensor calibration data, the final test bench has been used to load the sensor from three different orientations: a set of loads, increasing from 0.5 to 2.5 N has been imposed in the normal direction Z , and from 0.1 to 0.4 N in two shear loading configurations X and Y , each one along two sensor tether directions, as shown in Fig. 9. The loading force values were selected considering the sensor’s design and the simulation results, both reported in [3].

Given the vector of sensor piezoresistors fractional change in resistance $\Delta R/R$, oriented as shown in Fig. 9, and the corresponding vector of sensor loads F in Newton, the linear

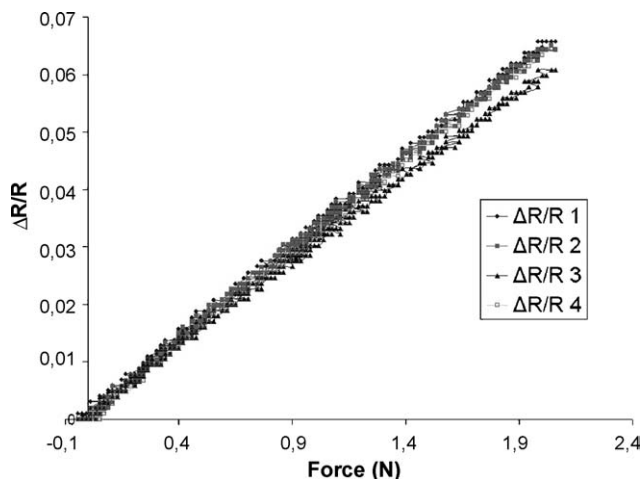


Fig. 7. $\Delta R/R$ vs. normal loading force.

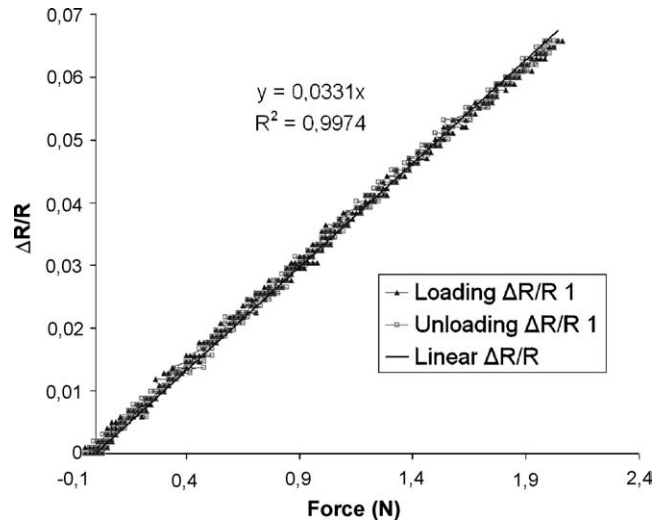


Fig. 8. $\Delta R/R$ vs. normal force in a hysteresis cycle.

transformation K between them in

$$F = K \frac{\Delta R}{R} \tag{2}$$

can be determined by evaluating the Moore-Penrose least-squares error solution to over determined set of equations. Using this method and the data collected during calibration, the final relationship between the piezoresistors fractional change in resistance and the applied forces becomes

$$K = \begin{pmatrix} -1.71 & 15.65 & -8.57 & -16.70 \\ -16.75 & 2.83 & 11.75 & 14.97 \\ 3.18 & 5.86 & 20.78 & 33.81 \end{pmatrix} N \tag{3}$$

The maximum errors of the sensor due to non-linearity when the least-squares transformation K is applied are 7 mN or 0.28% for the normal component of the force in the calibrated range (from 0 to 2.5 N) and 10 mN or 2.5% for the two shear components in the calibrated range (from 0 to 0.4 N).

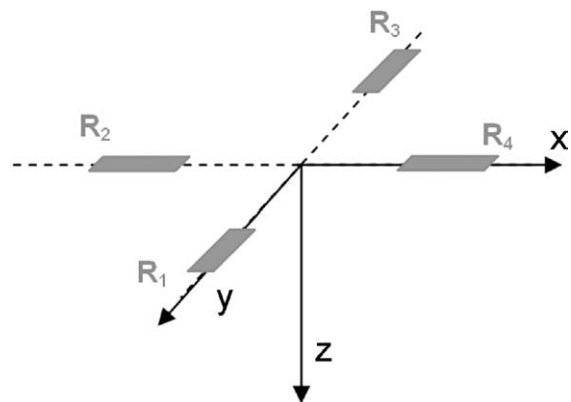


Fig. 9. Schematic design of the piezoresistors orientation.

Moreover, the experimental sensitivity matrix S_E , which is the Moore-Penrose pseudoinverse of matrix K , is

$$S_E = \begin{pmatrix} 0.0006 & -0.0540 & 0.0260 \\ 0.0540 & -0.0011 & 0.0260 \\ -0.0007 & 0.0077 & 0.0091 \\ -0.0090 & 0.0005 & 0.0170 \end{pmatrix} N^{-1} \quad (4)$$

Defining the sensitivity of the sensor as the largest in amplitude between the values obtained for the ratio of fractional resistance variation to the corresponding force, acquired for each of the four channels, then

$$S_x = \max_{i=1,\dots,4} \left(\left| \frac{(\Delta R/R)_i}{F_x} \right|_{F_y=F_z=0} \right) \quad (5)$$

$$S_y = \max_{i=1,\dots,4} \left(\left| \frac{(\Delta R/R)_i}{F_y} \right|_{F_x=F_z=0} \right) \quad (6)$$

$$S_z = \max_{i=1,\dots,4} \left(\left| \frac{(\Delta R/R)_i}{F_z} \right|_{F_x=F_y=0} \right) \quad (7)$$

From the experimental sensitivity matrix reported in (4), we obtain

$$S_x = S_y = 0.054 N^{-1} \quad (8)$$

$$S_z = 0.026 N^{-1} \quad (9)$$

During the calibration, several tests have been performed in order to assess the maximum loading force. The breaking normal load is around 3 N and the breaking shear load ranges from 0.5 to 0.7 N.

4. Discussion

In the sensitivity matrix S_E coefficients S_{E21} and S_{E41} relate the variation of the piezoresistors R_2 and R_4 to a load in the X direction. Results in (4) show that these two coefficients are opposite in sign, thus when the sensor is loaded with a tangential load in the X direction, R_2 is stressed and the R_4 is compressed. Moreover, being S_{E21} and S_{E41} larger than S_{E11} and S_{E31} , the applied load in the X direction has a low influence on R_1 and R_3 . The same can be stated for the second column of S_E , when loading the sensor along the Y direction. When a normal force is applied, all the four piezoresistors are stressed, thus the coefficients in third column of S_E are positive. In this case the values of the coefficients should be the same. Their differences in (4) are due to the tolerances of the various steps of both the sensor fabrication and assembly processes. For example, the flip-chip assembly process may cause a non-perfect alignment between the sensor and the carrier chips. Nevertheless, through the calibration procedure and the evaluation of the linear matrix transform between the piezoresistors signals and the force load vector, any non-ideality due to the processes is encompassed.

The sensitivity values reported in (8) and (9) were obtained without considering the electronic amplification that can be introduced during signal conditioning.

In order to make a comparison with the performances of most of the sensors reported in Table 1, in the sensitivity definition it is possible to consider the piezoresistors fractional change in resistance rather than the voltage output variation. Thus, we can define \tilde{S}_\bullet , that becomes as follows

$$\tilde{S}_x = \max_{i=1,\dots,4} \left(\left| \frac{V_i^{\text{out}}}{F_x} \right|_{F_y=F_z=0} \right) \quad (10)$$

and the same for the other force components. By substituting Eq. (1) into Eq. (10), it is possible to relate \tilde{S}_\bullet to S_\bullet , obtaining

$$\tilde{S}_x = \frac{A V_{IN}}{4} S_x \quad (11)$$

Thus, by using a low noise instrumentation amplifier, it is possible to increase up to 1000 times the sensitivity from S_\bullet to \tilde{S}_\bullet .

Moreover, since the signal source is a silicon p-type piezoresistor, it is possible to predict a noise spectrum with a $1/f$ Hooe noise, which dominates at the low frequencies, and a flat spectrum, due to the Johnson's or thermal noise, for frequencies greater than f_c . f_c is defined as the corner frequency, where the $1/f$ Hooe noise equals the Johnson noise [18]. Therefore, in order to minimize the signal noise, thus to increase the minimum force component resolvable by the sensor, the four Wheatstone bridges could be fed with a sinusoidal voltage supply V_{IN} , using a frequency greater than f_c .

5. Conclusions

The objective of this work has been the characterization of a miniature three-axial silicon based force sensor. A preliminary test bench has been developed, whose core component is a mono-axial load cell. Such a system allows to test the response linearity and sensor hysteresis, but it is not suitable for obtaining a reliable sensitivity matrix, since loading force vector can be acquired only for one of its three directions. Therefore, the characterization has been addressed with a more accurate and dedicated measurement system that, by means of a six-component load cell, permits complete sensor calibration through the application of arbitrary forces with known magnitude and direction.

The obtained results show a high linearity (99.7%) and the absence of hysteresis. The three components of the loading force have been acquired and related to the sensor output by a calibration matrix. From experimental data a sensitivity matrix has been obtained and sensitivities in the x , y and z directions have been identified as $S_x = S_y = 0.054 N^{-1}$ and $S_z = 0.026 N^{-1}$. The maximum force errors of the sensor using the calibration matrix are 7 mN for the normal component and 10 mN for the two shear components, both in the

calibrated force ranges. Experimental tests have also been performed in order to assess the maximum loading force: preliminary results show a breaking normal and shear load of around 3 N and from 0.5 to 0.7 N, respectively. Sensitivity values are very satisfactory if compared to the devices that are found in literature (see Table 1).

Future works will address the characterization of the same sensor complete with a flexible packaging suitable to implement a flexible smart interface for biomechanical measurements.

Acknowledgements

The research has been partially supported by the European Commission's "Improving Human Potential" (IHP) Program in collaboration with the Institut für Mikrotechnik Mainz (IMM), Germany. The authors wish to thank Mr. Carlo Filippeschi for his valuable technical support, and Dr. Ivano Izzo for valuable discussion.

References

- [1] L. Beccai, S. Roccella, A. Arena, A. Menciassi, M.C. Carrozza, P. Dario, Silicon-based three axial force sensor for prosthetic applications, in: Proceedings of the Seventh National Conference on Sensors and Microsystems, Bologna, Italy, February 4–6, 2002, pp. 250–255.
- [2] F. Valvo, P. Valdastrì, S. Roccella, L. Beccai, A. Menciassi, M.C. Carrozza, P. Dario, Development and characterization of a silicon-based three axial force sensor, in: Proceedings of the Ninth National Conference on Sensors and Microsystems, Ferrara, Italy, February 9–11, 2004.
- [3] L. Beccai, S. Roccella, A. Arena, F. Valvo, P. Valdastrì, A. Menciassi, M.C. Carrozza, P. Dario, Design and fabrication of a hybrid silicon three-axial force sensor for biomechanical applications, *Sens. Actuators A*, in press.
- [4] B. Massa, S. Roccella, R. Lazzarini, M. Zecca, M.C. Carrozza, P. Dario, Design and development of an underactuated prosthetic hand, in: Proceedings of the 2002 IEEE International Conference on Robotics and Automation, Washington, DC, USA, May 11–15, 2002, pp. 3374–3379.
- [5] M.C. Carrozza, P. Dario, F. Vecchi, S. Roccella, M. Zecca, F. Sebastiani, The CyberHand: on the design of a cybernetic prosthetic hand intended to be interfaced to the peripheral nervous system, in: Proceedings of the International Conference on Intelligent Robot and Systems, Las Vegas, NV, USA, October 27–31, 2003, pp. 2644–2647.
- [6] T. Mei, Y. Ge, Y. Chen, L. Ni, W.H. Liao, Y. Xu, W.J. Li, Design and fabrication of an integrated three-dimensional tactile sensor for space robotic applications, in: Proceedings of the 12th IEEE Int. Conf. MEMS, Orlando, FL, USA, January 17–21, 1999, pp. 112–117.
- [7] W.L. Jin, C.D. Mote, A six-components silicon micro force sensor, *Sens. Actuators A* 65 (1998) 109–115.
- [8] D.V. Dao, T. Toriyama, J.C. Wells, S. Sugiyama, Six-degree of freedom micro force-moment sensor for application in geophysics, in: Proceedings of the 15th IEEE Int. Conf. MEMS, Las Vegas, NV, USA, January 20–24, 2002, pp. 312–315.
- [9] L. Wang, D.J. Beebe, A silicon-based shear force sensor: development and characterization, *Sens. Actuators A* 84 (2000) 33–44.
- [10] S. Bütefisch, S. Büttgenbach, T. Kleine-Besten, U. Brand, Micromechanical three-axial tactile force sensor for micromaterial characterization, *Microsyst. Technol.* 7 (2001) 171–174.
- [11] M. Hsieh, Y. Fang, M. Ju, G. Chen, J. Ho, C.H. Yang, P. Wu, G.S. Wu, T. Chen, A contact-type piezoresistive micro-shear stress sensor for above-knee prosthesis application, *IEEE J. Microelectromech. Syst.* 10 (2001) 121–127.
- [12] B.J. Kane, M.A. Cutkosky, G.T.A. Kovacs, A traction stress sensor array for use in high-resolution robotic tactile imaging, *J. Microelectromech. Syst.* 9 (2000) 425–434.
- [13] Z. Chu, P.M. Sarro, S. Middelhoek, Silicon three-axial tactile sensor, *Sens. Actuators A* 54 (1996) 505–510.
- [14] Z. Chi, K. Shida, A new multifunctional tactile sensor for three-dimensional force measurement, *Sens. Actuators A* 111 (2004) 172–179.
- [15] P.J. Berkelman, L.L. Whitcomb, R.H. Taylor, P. Jensen, A miniature microsurgical instrument tip force sensor for enhanced force feedback during robot-assisted manipulation, *IEEE Trans. Robot. Automat.* 19 (2003) 917–921.
- [16] D. Diddens, D. Reynaerts, H. Van Brussel, Design of a ring-shaped three-axis micro force/torque sensor, *Sens. Actuators A* 46 (1995) 225–232.
- [17] W.L. Jin, C.D. Mote, Development and calibration of a sub-millimeter three-component force sensor, *Sens. Actuators A* 65 (1998) 89–94.
- [18] J.A. Harley, T.W. Kenny, 1/f noise considerations for the design and process optimization of piezoresistive cantilevers, *J. Microelectromech. Syst.* 9 (2000) 226–235.

Biographies

Pietro Valdastrì received his Laurea Degree in Electronic Engineering (with Honors) from the University of Pisa in February 2002. In the same year he joined the CRIM Lab of the Scuola Superiore Sant'Anna in Pisa as a Research Assistant. In January 2003 he started his PhD in Bioengineering at CRIM Lab. Main research interests are in the field of implantable biotelemetry, MEMS-based biosensors, and swarm robotics. He is working on several European projects for the development of minimally invasive biomedical devices.

Stefano Roccella received his Laurea Degree in Aeronautical Engineering from the University of Pisa in February 1999. In the same year he joined the Advanced Robotic Technology and System (ARTS) Laboratory of the Scuola Superiore Sant'Anna in Pisa as a Research Assistant. In March 2003 he started his PhD in Robotics at University of Genova. Currently he is an assistant professor of biomedical robotics at Scuola Sant'Anna, where he is member of the ARTS Lab. His research interests are in the fields of biomedical robotics, rehabilitation engineering, biomechanics and MEMS design and development.

Lucia Beccai received her Laurea Degree in Electronic Engineering from the University of Pisa in February 1998. She joined the Center of Research in Microengineering (CRIM, formerly MiTech) Laboratory in June 1999 as Research Assistant. She received her PhD degree in Microsystem Engineering in March 2003 by discussing a thesis entitled "Design, fabrication and packaging of a silicon based three-axial force sensor for biomedical applications" and now has a post-doctoral position at the CRIM lab of Scuola Superiore Sant'Anna. She collaborates to several European projects and her research interests are in the fields of micro-fabrication technologies, microsystems for biomedical applications, and sensory systems' integration in robotics and rehabilitation engineering.

Emanuele Cattin received his Laurea Degree in Mechanical Engineering from the University of Padova in July 2003. Since April 2004 he joined the Advanced Robotic Technology and System (ARTS) Lab of the Scuola Superiore Sant'Anna in Pisa as a Research Assistant. His main research interests are in the fields of robotics, mechatronics, biomechanics, prosthesis and biomechanics.

Arianna Menciassi received her Laurea Degree in Physics (with Honors) from the University of Pisa in 1995. In the same year, she joined the CRIM (formerly MiTech) Lab of the Scuola Superiore Sant'Anna in Pisa as a PhD student in bioengineering with a research program on the micromanipulation of mechanical and biological micro-objects. In 1999, she received her PhD degree by discussing a thesis titled "Microfabricated Grippers for Micromanipulation of Biological and Mechanical Objects". She had a post-doctoral position at SSSA from May 1999 until April 2000. Then, she obtained a temporary position of assistant professor in bioengineering at SSSA. Her main research interests are in the fields of biomedical microrobotics, microfabrication technologies, micromechanics and microsystem technologies. She is working on several European projects and international projects for the development of minimally invasive instrumentation for medical applications.

Maria Chiara Carrozza received her Laurea Degree in Physics from the University of Pisa in 1990, and the PhD degree in mechanical engineering at Scuola Superiore Sant'Anna, Pisa, in 1994. Currently, she is an associate professor of biomedical robotics at Scuola Sant'Anna, where she directs the Advanced Robotic Technology and System (ARTS) Laboratory. She is also the scientific manager of the research area of functional replacement at the INAIL/RTR Research Center on Rehabilitation Engineering. Her research interests are in the fields of biomedical microengineering and rehabilitation engineering. She is a member of the

IEEE Engineering in Medicine and Biology and IEEE Robotics and Automation Societies.

Paolo Dario received his Laurea Degree in Mechanical Engineering from the University of Pisa in 1977. Currently, he is a professor of biomedical robotics at the Scuola Superiore Sant'Anna, Pisa. He also established and teaches the course on mechatronics at the School of Engineering, University of Pisa. He has been a visiting professor at the Ecole Polytechnique Federale de Lausanne (EPFL), Lausanne, Switzerland, and at Waseda University, Tokyo, Japan. He is the director of the Center for Research in Microengineering Laboratory of SSSA, where he supervises a team of about 70 researchers and PhD students. His main research interests are in the fields of medical robotics, mechatronics and microengineering, and specifically in sensors and actuators for the above applications. He is the coordinator of many national and European projects, the editor of two books on the subject of robotics and the author of more than 200 scientific papers. He is a member of the Board of the International Foundation of Robotics Research. He is an associate editor of the IEEE Transactions on Robotics and Automation, a member of the Steering Committee of the Journal of Microelectromechanical Systems and a guest editor of the Special Issue on Medical Robotics of the IEEE Transactions on Robotics and Automation. He serves as president of the IEEE Robotics and Automation Society and as the co-chairman of the Technical Committee on Medical Robotics of the same society.